Core rearrangement of excited atomic states near a metal surface and adsorbate effects

1994 J. Phys.: Condens. Matter 6 L699

(http://iopscience.iop.org/0953-8984/6/45/003)

J. Phys.: Condens. Matter 6 (1994) L699–L707. Printed in the UK

LETTER TO THE EDITOR

Core rearrangement of excited atomic states near a metal surface and adsorbate effects

V A Esaulov

Laboratoire des Collisions Atomiques et Moléculaires (Unité Associée au CNRS), Bâtiment 351, Université de Paris Sud, 91405 Orsay, France

Received 8 September 1994

Abstract. A mechanism of the core rearrangement of excited atomic states near a metal surface is presented. A numerical model is developed and applied to the description of the rearrangement of ^{1}D core states of Ne** and Ne^{+*} to ^{3}P core states. This is ascribed to resonant ionization of ^{1}Dnl states into the continuum: Ne^{++}(^{3}P)+metal, followed by resonant electron capture. This ionization is rendered possible by level shifts near a metal surface. Effects of adsorbates are investigated and it is shown that a lowering of the workfunction induces a strong decrease of the rearrangement.

Recent experimental studies of ion–surface interactions have revealed the existence of a most interesting possibility of rearrangement of atomic states near a metal surface, processes of fundamental interest for surface chemistry. Thus a conversion from He(2 ^{1}S) to He(2 ^{3}S) metastable atoms near a metal surface was recently reported [1]. This was described [2] in terms of electron capture and loss processes involving the He^{-*} (1s 2s^{22}S) Fechbach resonance. This process involves outer electrons. The existence of another type of rearrangement process involving *core* electrons has recently been suggested. Its existence was inferred [3–7] from a comparison of the characteristics of autoionizing state production in the scattering of Ne ions and atoms on Mg and Al surfaces, with previously studied gas-phase collisions of Mg^+ and Al^+ with Ne [8–10]. The autoionizing states considered are: Ne**(2p^4 (^{3}P) 3s^2) and Ne**(2p^4 (^{1}D) 3s^2). Production of these states was attributed to 'binary' collisions, of incident Ne and a surface Mg atom, and described [3–6] in terms of transitions between states of a transient quasimolecule, using a molecular orbital correlation diagram as for an atom–atom case [8, 9]. In gas-phase collisions of Mg^+ with Ne, dominant production of the ^{1}D core states [4, 8] is observed, whereas in Ne scattering on solid Mg, Ne**(^{3}P 3s^2) is dominant. Assuming that, in ion–solid collisions, the primary electron promotion mechanisms remain valid, it was suggested that the triplet core dominance is due to core rearrangement [3–7]. This is also known to exist in gas-phase [9] collisions and a small amount of triplet core formation in Al^+ collisions with Ne has been reported [10]. A similar two-electron Auger-type quasimolecular mechanism could also exist here [3, 5], though it seems doubtful that this could lead to such a strong triplet production. Experimental tends support *surface-induced enhanced* rearrangement [3, 5, 6, 11]. Existing data show that dominance of Ne** (^{3}P 3s^2) corresponds to low perpendicular exit velocities ($v_\perp$) i.e. longer dwelling times near the surface. It is also found that adsorbates strongly affect the singlet to triplet core ratios and it was concluded that the rearrangement process is affected by adsorption [5]. Thus, initial stages of oxidation result in a dramatic drop of the

0953-8984/94/450699+09$19.50

triplet to singlet peak ratios and lead to their disappearance at higher coverages [4, 5]. In the case of Na adsorption one first observes a drop in this ratio, which, however, increases again at larger coverages [7]. The overall intensity of both peaks increases in the higher-coverage range. In the case of Na adsorption, the workfunction (ϕ) decreases. In the case of the Mg target a strong decrease of ϕ is also observed for oxygen adsorption, whereas for Al this only produces a small decrease [5].

The above effects were initially tentatively assigned to an enhancement of the quasimolecular rearrangement by metal electrons [3, 5–7]. However, this explanation did not seem to be an entirely satisfactory one. Firstly, the energetics of this process, i.e. the position of the relevant energy levels of the quasimolecule in front of the surface, is not known. Secondly, this Auger-type process, involving transitions between molecular states and an electron from the metal band, would only be efficient after the primary excitation had occurred, for the short duration of the separation of the quasimolecule's constituents, in an internuclear range of about one ångström ($\sim 10^{-15}$ s for 1 keV Ne). One wonders about its efficiency, and one can come to doubt the implicit (and arbitrary) assumption of the validity of the basic electron promotion picture, which, on the other hand, seems to be supported by general experimental trends [5] of excited state production. The questions we ask ourselves are then: is there really a case for a surface-enhanced core rearrangement process and if so, can a mechanism be found that will account for the experimental observations and allow us to account for the major difference between atom–solid and atom–atom collisions, which otherwise could be considered as a major failure of the gas-phase description here.

In this letter we propose a mechanism of this metal-induced core rearrangement process, which is active *after* the small-impact-parameter 'binary' collision has occurred, as the excited species leaves the surface. It is thus operative over a larger range of distances. We present computer simulations for some model situations, in which we reproduce, qualitatively, known experimental trends and hence give a reason for reconciling the difference between the gas-phase and ion–solid collisions with the electron promotion mechanism.

It should be noted that the new mechanism we propose is actually much more *general* and should play a role in the rearrangement of atomic states of many elements with incomplete outer shells, for which there exist several core states. This is the case of most common adsorbates such as oxygen. It will also appear in the neutralization of highly charged ions at surfaces. Our analysis is furthermore of interest in understanding ion production in a SIMS situation.

We consider what happens when a Ne atom (or ion) in an excited ^{1}D$nln'l'$ (or ^{1}D nl) state or Ne^{++}(^{1}D), produced in a violent encounter with a surface atom, for small atom–atom separations, leaves the surface in a range of exit angles θ_{ex} and energies (E_{ex}) governed by the 'binary' collisional event and deflections by other surface atoms. We attribute rearrangement to ionization into the continuum represented by: metal + Ne^{++}(^{3}P), followed by electron capture processes. This ionization is the *analogue of the autoionization of open shell atoms in their free states.* In the case of these atoms we also deal with systems with several core states. Most singly excited states of the higher Rydberg series, e.g. F((2p^4)^{1}D nl) lie 'naturally' above the F$^+$((2p^4)^{3}P) continuum and autoionize [12]. In the case of Ne, most ^{1}D core states lie *below* the ^{3}P Ne^{++} continuum limit. However when we consider an atom or ion near a metal surface, we must consider level shifts induced by image charge effects, due to which excited state levels will lie above the Fermi level at small distances. Actually a level can be bound with respect to its parent continuum: metal + Ne^{++} (^{1}D) (MDC), *but be autoionizing with respect to the continuum*: metal + Ne^{++}(^{3}P) (MPC). This is crudely schematized in figure 1. An excited atom or ion formed collisionally

in the ^1Dnl configuration can thus autoionize into its parent *and* into the ^3P core related continuum. The resulting $Ne^{++}(^3P)$ or $Ne^{+*}{}^3Pnl$ can then capture electrons giving the final state distribution. Note that autoionizing states such as $Ne^{**}(^1D\ 3s^2)$ can decay into $Ne^{+*}(^3Pnl)$, a process observed by us in, e.g., F^{-**} $(^1D\ 3s^2)$ autodetachment [13].

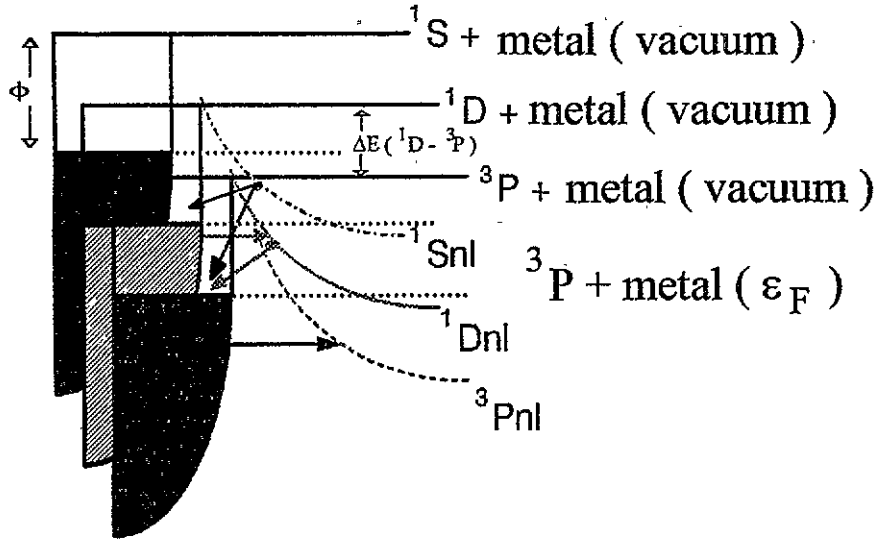

Figure 1. Schematic diagram of the rearrangement process, showing the three metal + atom ($2p^4$) systems, level shifts, intracore (horizontal arrow) and intercore (sloping arrow) transitions.

In order to delineate the characteristics of this process we now present a numerical simulation of the transformations which affect the initially produced excited species. Here we have to consider a series of Auger and resonant capture and loss processes involving each parent continuum *and other continua.* Because of the complexity of the problem, and the number of states involved, it is not possible to perform exact calculations. We adopt a *model* simplified reaction scheme shown in figure 2 for a given excited state. We limit the modelling to the consideration of the $Ne^{**}(^3P\ 3s^2/3p^2)$, $Ne^{**}(^1D\ 3s^2/3p^2)$, $Ne^{+*}(^3P\ 3s/3p)$ and $Ne^{+*}(^1D\ 3s/3p)$ states and replace the actual manifold of levels by the lowest terms. For the unknown starting conditions we shall consider the following combinations: (a) Ne^{++} ^1D; (b) 50% Ne^{+*} $(^1D\ 3s)$ and 50% $Ne^{+*}(^1D\ 3p)$ states and finally (c) 50% Ne^{**} $(^1D\ 3s^2)$ and 50% Ne^{**} $(^1D\ 3p^2)$ states. Initial population of the triplet core state in the collision is not considered. We assume that these species start out at a distance of 1 atomic unit from the image plane. The initial choice of a small starting distance seems reasonable, since the excited states are created at small atom–atom separations. We consider the ejection of excited particles into a range of θ_{ex}, with E_{ex} corresponding to energy losses in single-scattering conditions. These starting conditions, and the parameters used in the following, allow us to delineate qualitatively some of the most important characteristics of the final state distributions. Only key features are described here, while a more detailed account of this work will be presented elsewhere.

We use a numerical model built along the lines of [14], with some small differences. Figure 3(a) shows the metal + atom/ion states corresponding to the above states and the scheme in figure 2. The construction of these follows a procedure described in some detail in

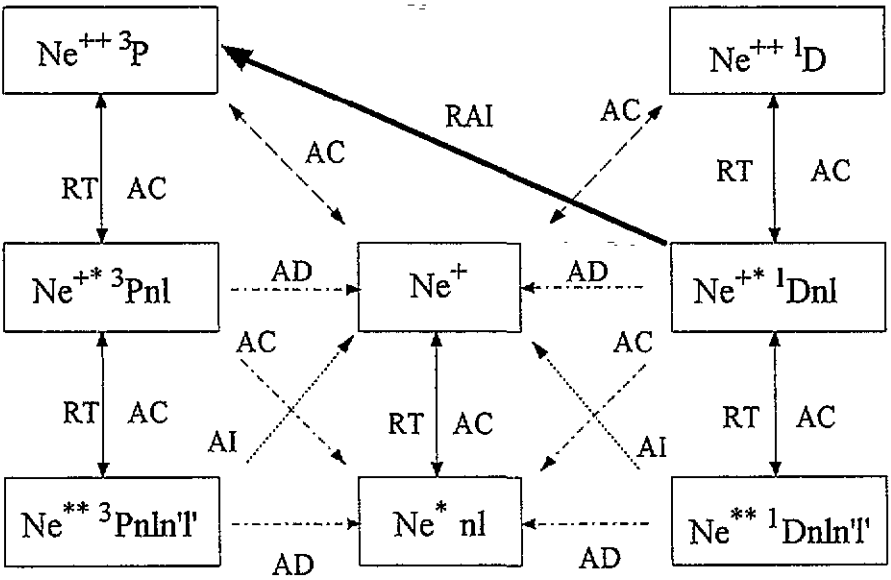

Figure 2. Electron loss and capture scheme between various Ne^{++}, Ne^{+}, Ne states. The various Auger capture (AC), Auger de-excitation (AD), resonant transfers (RT), autoionization (AI) and rearrangement (RAI) channels between states are indicated. The excited states actually considered are given in the text.

[14], and takes into account both image potential effects and screening at small atom–surface distances. Note the crossing of the Ne^{+*} (^1Dnl) levels with the MPC limit. The crossing of the 3s level occurs at a small atom–surface distance, while that of the higher-lying 3p one, at larger distances.

We solve a set of coupled differential equations for the distance dependent populations of the various levels.

$$\frac{dN_i}{dz} = \left[\sum_{i\neq k}(G_{ki}(z)N_k(z) - G_{ik}(z)N_i(z))\right]\Big/ v_\perp$$

where $G_{ik}(z)$ are the probabilities for transition between i and k states. We assume [14] that the resonant and Auger transitions are caused by the overlap of the wavefunctions of the electron in its initial and final state and that $G_{ik}(z)$ is determined by the asymptotic behaviour of the wavefunctions. For resonant electron transfers (and resonant ionization)

$$G_{ik}(z)_{RT} = C_{RT}\rho(E_b)\exp\left[-\left(\sqrt{2E_{ik}(z)}\right)z\right]$$

where $E_{ik}(z)$ is the binding energy of the electron in state i with respect to its parent state k, C_{RT} is an adjustable parameter, and $\rho(E_b)$ is the metallic density of states (DOS), which is normalized to unity. The parameters chose subsequently should be related to this normalization. For resonant capture $E_b = E(z)$. Our inclusion of $\rho(E)$ reflects the fact that resonant neutralization should in some way depend on the 'availability' of electrons of a given energy. For the case of resonant ionization $\rho(E) = \rho(\epsilon_F)$, where ϵ_F is the Fermi energy. For Auger capture and de-excitation $G_{ik}(z)$ is defined [14] as an integral over the

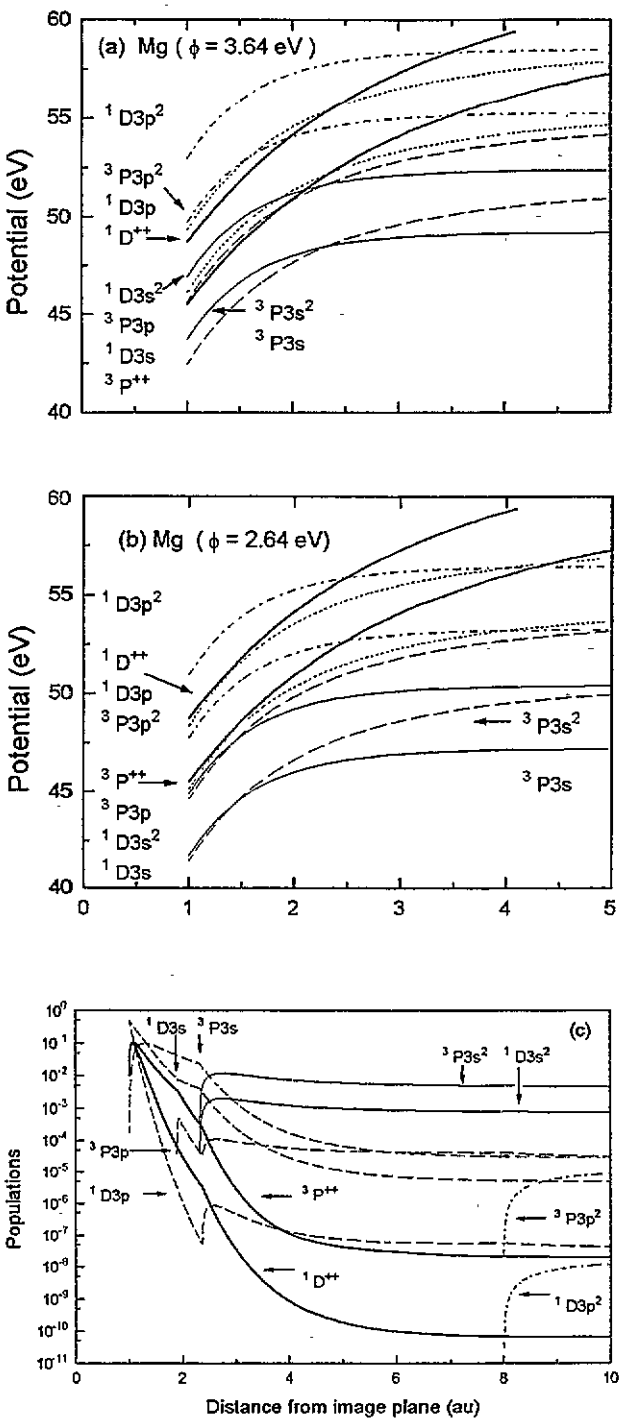

Figure 3. (a) Potential energy diagram of the Ne–Mg system used in the calculations (f = 3.64 eV) represented here for electrons at the Fermi level. The states are identified on the left of the diagram. The thick lines represent the Ne^{++} + metal continuum. (b) Same, but for f = 2.64 eV. (c) Populations of the various states as a function of the distance from the image plane (f = 3.64 eV, q_{ex} = 27°, E_{ex} = 1.55 keV).

binding energies of metal electrons in the band,

$$G_{ik}(z) = \int_{\epsilon_{min}}^{\epsilon_F} \rho(E_b) C_{AC} \exp\left[-z\left(\frac{1}{2\sqrt{2E_b(z)}} + \frac{1}{2\sqrt{2E_a(z)}} \right)^{-1} \right] dE_b$$

where E_a is the recombination energy of the atomic electron. We also consider Auger capture into excited states and hence the lower limit in the above integral is not necessarily zero and is determined by the position of the level with respect to the band. In this case the E_a is the binding energy of the electron in state i with respect to its parent state k. In the case of the filling of the inner 2p hole in neutralization and de-excitation, E_a was taken as the ionization potential of the atom. C_{AC} is an adjustable parameter.

A jellium band structure was used. The autoionization of the doubly excited atom into the ground state of the ion is assumed to be given by a distance independent parameter, chosen as 0.0005 au as for He^{**} and Ar^{**} [14], which corresponds to a lifetime of about 5×10^{-14} s. No attempt at deriving the values of all parameters from any fitting procedure as in [14] was made, since we are only interested in a qualitative description of the main experimental trends. We make the simplifying assumption that capture into $Ne^*(3s)$ leads to only $Ne^{**}(3s^2)$ formation and similarly $Ne^*(3p)$ leads to only $Ne^{**}(3p^2)$. This is contrary to [14], where it was assumed that capture by $Ar^{+*}(3p)$ leads to $Ar^{**}(3s^2)$, but this capture mechanism is not clear. Most C parameters were equated for simplicity and the following set, based on the parameters of [14] for the Ar^{++}/Pb system, was used (in atomic units).

(i) Auger capture (e.g. $Ne^{++} \rightarrow Ne^{+}$): 0.4.

(ii) Auger de-excitation (e.g. $Ne^{**} \rightarrow Ne^{*}$): 0.2.

(iii) Resonant neutralization and ionization: 0.05 (note that: $0.05\rho(\epsilon_F) \cong 0.3$).

(iv) Resonant autoionization leading to rearrangement (^1D 3s/3p $\rightarrow Ne^{++}(^3P) + e^-$): 0.025. This value was chosen to give the experimental order of magnitude of the triplet to singlet ratio.

Results of the calculation of the distance dependent populations of the various levels are schematized in figure 3(c) for 2 keV Ne incident at 6° grazing angle (α) to the surface and scattered through 33° ($E_{ex} = 1.55$ keV and $\theta_{ex} = 27°$). Note that because at a distance of 1 au most ionic and atomic states lie above the Fermi level, the initial population of the Ne^{+*} (^{1}D3s, 50% and ^{1}D 3p, 50%) states drops rapidly with increasing z, resulting in the formation of Ne^{++}(^{3}P and ^{1}D). This is followed by electron capture *resulting in particular in the formation of the ^3P nl and ^3P nl n'l'states*. The final populations of the Ne^{**} ($3s^2$) states corresponding to the two cores are given in figure 4, for several E_0 and in a range of θ_{ex}. Note that a less than 1% fraction of the $^3P(3p^2)$ state is expected, which is in agreement with experiment [11, 15].

The main features of our results, common to Mg and Al, are determined by the *time spent near the surface and are related to the greater survival of the intial state for high E_{ex}*. These are as follows.

(a) The resultant intensity of Ne^{**} is larger for higher E_0.

(b) For a given E_0 the ratio (R_{ts}) of the triplet to singlet core states decreases as θ_{ex} and E_{ex} increase. The drop in maximum intensity and a reincrease of the ratio for angles beyond 45° is due to the lowering of $v_\perp$. The angular distribution of the triplet core state will onset at smaller angles than the singlet core state as shown experimentally in [6] for an Al target. The model and experimental [6] singlet to triplet core ratios ($1/R_{ts}$) are shown in figure 4(d).

(c) R_{ts} decreases as E_0 increases, in agreement with experiment [3, 11], where this ratio for integral peak intensity is about 5 for 500 eV and 2.5 for 2 keV.

These qualitative features do not change when we consider the other initial state distributions mentioned above. In the case of initially populated Ne^{**} states, resonant ionization into Ne^{+*} leads to a situation similar to the one with initially populated Ne^{+*}.

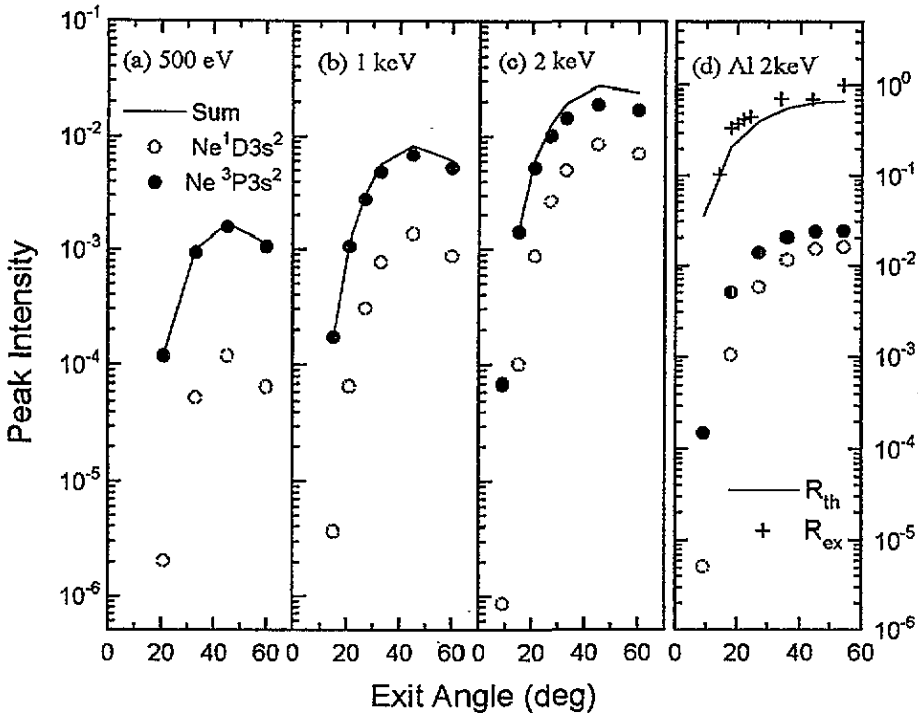

Figure 4. (a)–(c) Exit angle dependence of the intensity of atoms scattered from Mg in the $3s^2$ states, for different collision energies ($\alpha = 6°$). (d) Same for Al at 2 keV. Experimental [6] (R_{ex}) and model (R_{th}) singlet to triplet ratios are also shown.

When we start with Ne^{++} (^{1}D) rearrangement occurs, because of an initial capture into Ne^{+*} (^{1}D 3s/3p), which then leads to ionization into MPC. The main difference is that the final intensity is lower, because of immediate competition from Auger neutralization, whereas for the excited states this onsets after ionization. Changes in the values of the parameters used led to changes in the absolute magnitude of the rearrangement process, but did not alter the main trends. The increase of the starting distance obviously leads to a decrease in the efficiency of rearrangement, since the range over which the process occurs decreases.

Thus our model reproduces the experimentally observed trends in the core rearrangement process for the clean metal target. Let us now consider cases of adsorption and first consider the effect of reducing the workfunction.

The most obvious effect will be the *stabilization* of all states against resonant ionization. Figure 3(c) shows the metal–atom states for a reduced $\phi(\Delta\phi = -1$ eV). Note that the $Ne^{+*}(^1D)3s$ state is now '*stabilized*', i.e. lies below the MPC limit in a much larger range of distances and hence *does not participate as efficiently in the rearrangement* process. The Ne^{**} (^{1}D)$3s^2$ state is also stablized down to small distances. It is clear from figure 3(b) that given the 'precarious' position of the Ne^{+*1}D3s state, as soon as ϕ starts to decrease, a decrease in the intensity of the triplet core states should occur. At the same time one can expect effects due to the stabilization of Ne^{**} (^{3}P) $3s^2$ and other states. Figure 5 shows the modifications in the calculated ratio of ^{3}P $3s^2$ to the sum ^{3}P $3s^2$+ ^{1}D $3s^2$ for a 27° exit angle. Qualitatively similar behaviour is observed at other angles. A dramatic decrease of this ratio is observed in the initial stages of the decrease of ϕ. The other interesting effect is that, after an initial violent drop, this ratio increases somewhat for $\Delta\phi$ greater than

0.5 eV and then decreases again slowly. We relate this to a succession of stabilizing factors. Initially, while the Ne^{+**} $^1D(3s)$ state is becoming rapidly stabilized, the 3p and $3s^2$ states of both cores are not yet strongly affected. However for larger decreases of ϕ, these are also stabilized. For $\phi < 2.64$ eV the ^1D 3p state becomes stable with respect to its parent continuum. At this stage we witness another drop in the conversion ratio. In the case of the Al target a similar behaviour is observed, but because of the higher ϕ, the minimum is observed at a higher $\Delta\phi$ of about 1.1 eV (figure 5). These observations are consistent with the experimental findings [5, 7]. In [7], a minimum for the Al target is observed for $\Delta\phi$ of the order of 1 eV, suggesting that the energy levels are reasonably modelled here.

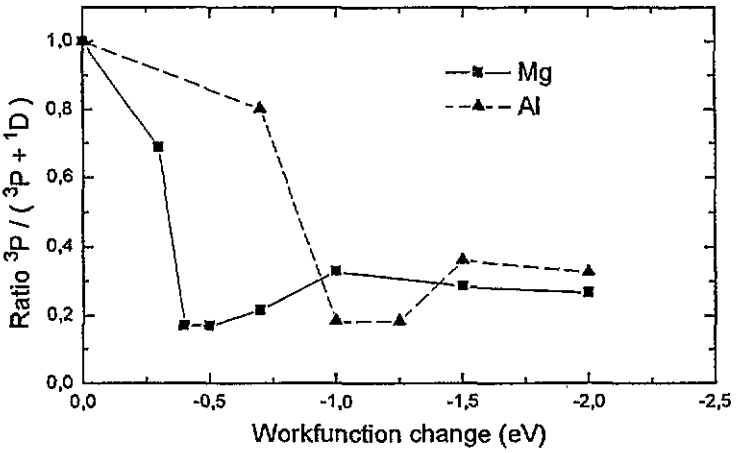

Figure 5. Variation of the normalized ratio of the ^3P to ^1D core $3s^2$ states for 2 keV ions incident at 6° for a 27° exit angle, as a function of workfunction decrease for a Mg ($f = 3.64$ eV) and an Al ($f = 4.25$ eV) target.

We noted above that the total intensity of the autoionizing states decreases upon oxygen adsorption [5] and increases in the case of Na [7]. An important factor, which plays a role in the observed changes in intensity, is collisions with both target metal and adsorbate atoms as discussed by us previously [5]. In the case of oxygen atoms, we do not expect Ne^{**} production [5, 12]. In the case of Na, Ne^{**} state production is known to be not only efficient, but more efficient, than for Mg (or Al) [8–10] at the low energies of the experiment of [7]. The experimental results can be understood in view of these different characteristics of collisions with the two adsorbate atoms.

Our model of the core rearrangement process is found to be in good qualitative agreement with experiment. The proposed process, which is active *after* the 'binary' collision has occurred, gives a good reason for reconciling the difference between the gas-phase and ion–solid collisions with the electron promotion mechanism. This mechanism, based on resonant autoionization of excited atoms corresponding to the higher core state, into the lower-core-state ion + metal continuum, followed by electron capture processes, is very general and should play a role in the rearrangement of atomic states of many open shell elements, such as the most common adsorbates. Theoretical studies of the various components of this rearrangement sequence: the electronic states of the system and electron transfe rates would be most helpful in rendering the above model quantitative. Calculations of the proposed resonant autoionization with core rearrangement rates would be particularly intersting.

The author is grateful to F Zu and R Baragiola for communication of experimental results prior to publication. Interesting discussions with them and I Urazgildin are gratefully acknowledged. Thanks are due to J P Gauyacq for comments on the manuscript.

References

[1] Brenten H, Müller H and Kepter V 1992 *Z. Phys.* D **22** 563
[2] Hemmen R and Conrad H 1991 *Phys. Rev. Lett.* **67** 1314
Borisov A G, Teillet-Billy D and Gauyacq J P 1993 *Surf. Sci.* **284** 337
[3] Zampieri G, Meier F and Baragiola R 1984 *Phys. Rev.* A **29** 116
[4] Lacombe S, Guillemot L, Huels M, Vu Ngoc Tuan and Esaulov V A 1993 *Surf. Sci.* **295** L1011
[5] Esaulov V A, Guillemot L and Lacombe S 1994 *Nucl. Instrum. Methods Phys. Res.* B at press
Lacombe S, Guillemot L and Esaulov V A 1994 *Surf. Sci.* **304** L431
[6] Lacombe S, Guillemot L, Huels M, Vu Ngoc Tuan and Esaulov V A 1994 *Izv. Russ. Acad. Sci* at press
[7] Xu F, Mandarino N, Zoccoli P and Bonanno A, Oliva A and Baragiola R 1994 *Phys. Rev. Lett.* submitted
[8] Fayeton J, Anderson N and Barat M 1976 *J. Phys. B: At. Mol. Opt. Phys.* **9** L149
[9] Olsen J O, Anderson T, Barat M, Courbin-Gaussorgues Ch, Sidis V, Pommier J, Agusti J, Andersen N and Russek A 1979 *Phys. Rev.* A **19** 1457
[10] Dowek D 1978 *Thesis* Université de Paris Sud
[11] Lacombe S, Guillemot L and Esaulov V A to be published
[12] Boumsellek S and Esaulov V A 1990 *J. Phys. B: At. Mol. Opt. Phys.* **23** 1303, 279
[13] Grouard J P, Esaulov V A, Hall R I, Montmagnon J L and Vu Ngoc Tuan 1986 *J. Phys. B: At. Mol. Opt. Phys.* **19** 1483
[14] Eeken P, Fluit J M, Niehaus A and Urazgildin I 1992 *Surf. Sci.* **273** 160
[15] Gallon T E and Nixon A P 1992 *J. Phys.: Condens. Matter* **4** 9761